H53D-0885 Numerical simulation of fluid flow in a single fracture under loading and unloading conditions (Enhanced Version)

Tobias Kling[1], Da Huo[2], Jens-Oliver Schwarz[3], Frieder Enzmann[3], Philipp Blum[1], Sally Benson[2]

[1]Karlsruhe Institute for Technology (KIT), Institute for Applied Geoscience (AGW), Kaiserstraße 12, 76131 Karlsruhe, Germany
[2]Stanford University, School of Earth Sciences, 397 Panama Mall, Mitchell Building 101, Stanford, CA 94305-2210
[3]Johannes Gutenberg University of Mainz, Institute for Geosciences, J.-J.-Becher-Weg 21, 55128 Mainz, Germany

Contact information:
Tobias Kling, M.Sc.
PhD student
tobias.kling@kit.edu
Tel: +49 721 608 45686

1. Introduction

Fluid flow in fractures is of particular importance in a wide range of geological disciplines (e.g. geothermal energy, hydrocarbons, CO_2 storage). Over decades, several scientists have been concerned with fluid flow in fractured rocks by considering analytical (e.g. [6]) as well as numerical (e.g. [5]) approaches. The main objective of the current study is the forward modelling of stress-dependent, single-phase fluid flow in a synthetically fractured sandstone by using the Lattice-Boltzmann-Brinkman method solving the incompressible Navier-Stokes-Brinkman equation. In addition, the simulations are expected to provide better insight into stress-dependent fluid flow behaviour in fractured, porous media represented by a heterogeneous, low-porosity sandstone. The model setup is based on medical CT scans simultaneously conducted during a core flooding experiment with progressively increasing and subsequently decreasing confining pressures enabling validation of the simulations.

2. Material and methods

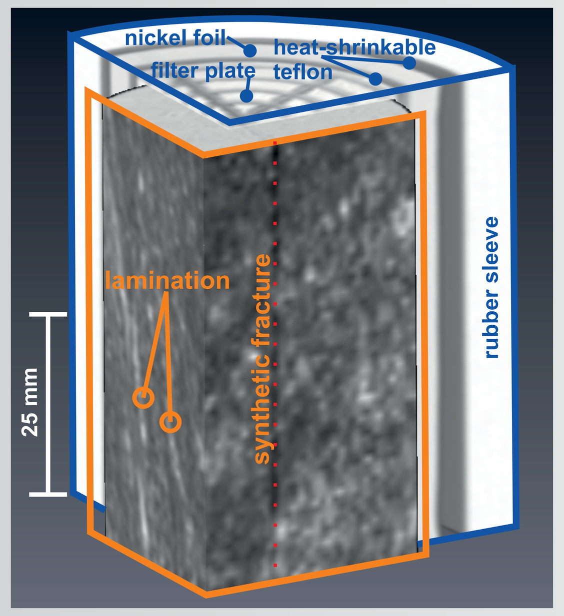

Fig. 1: CT image (0.25 x 0.25 x 0.25 mm³) of the fractured rock sample (orange) and setup of the core holder interior (blue).

Table 1: Description and matrix properties of the rock sample (orange = used as boundary condition of the model)

Core Sample	
Description	Precambrian Zenifim Sandstone (Ramon-1 well, Negev/Israel)
Background	Influences of fractures in non-permable sedimentry rocks
Lithology	Highly-cemented, immature, heterogenous greywacke
Core size [cm]	Length = 6.7; Diameter = 5
Porosity [%]	2.5 to 3.9
Permeability [mD]	0.0006 (= $5.9e^{-19}$ m²)
CT_{mat} [HU]	1862.6 (= CT number of matrix rock)
Fracture type	Synthetic, saw-cut fracture

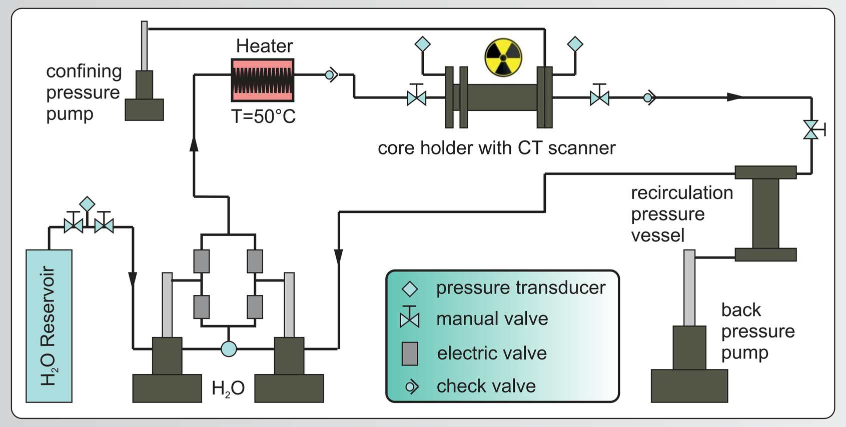

Fig. 2: Schematic setup and functionality of the core flooding apparatus (after [2]).

Table 2: Experimental conditions (orange = used as boundary condition of the model)

Fluid	Pure H_2O (50°C)
Fluid viscosity [Ns/m²]	$4.5e^{-4}$
Flow rates [ml/min]	12, 16, 20
Pore pressure [MPa]	2.07
Confining Pressures [MPa]	0.69, 2.07, 3.45, 5.52, 11.03, 22.06
Measurement	Pressure drop/ Permeability K (by using Darcy's law)

In a **core flooding experiment** (Fig.2) the permeability of a synthetically fractured, heterogeneous sandstone sample (Fig.1) has been measured under increasing and decreasing confining pressures. In-situ scans with a **medical X-ray computer tomography (CT) scanner** (voxel: 0.5 x 0.5 x 1 mm³) provide the geometry of the sample for the model setup. For each pressure stage, five CT scans were averaged to enhance the resolution according to the **missing attenuation method** (MAM) [4]. Afterwards, the processed image was rescaled to a voxel dimension of 0.25 x 0.25 x 0.25 mm³. Simulations were performed using the commercial software program package **GeoDict®** [1] on a SuperMicro Platform (64 cores, 512 GB RAM). Fluid flow is simulated using the single-phase **Lattice-Boltzmann-Brinkman (LB) method** solving the incompressible **Navier-Stokes-Brinkman equation**. The simulated fluid velocities are transfered to permeabilities assuming the local cubic law. Boundary conditions are given by experimental data (Table 1 & 2). Additionally, two artifical filter plates (K = $1e^{-10}$ m²) are attached to the core endings to provide a homogenous inflow and outflow zone.

3. Results and discussion

Experiment

Hysteretical behaviour of, both, permeability and aperture under loading and unloading conditions implies a causal relationship (Fig. 3).

- Permeabilities significantly decrease with increasing confining pressures from $1.77e^{-12}$ m² (0.69 MPa) to $5.87e^{-14}$ m² (22.06 MPa).
- Mean apertures also decrease with increasing confining pressures and are significantly smaller (ca. 25 - 30 microns) than applied spacer widths (Fig.4).

Simulation

- First simulations for the lowest and highest loading conditions reveal permeabilities of $9.43e^{-13}$ m² (at 0.69 MPa) and $6.78e^{-13}$ m² (at 22.06 MPa).
- The simulated permeabilities do not exactly fit with the corresponding measured data, but are situated between both measured extrema and indicate reduction with increasing confining pressures.
- Fluid flow occurs along conduits within the fracture and, partially, within the matrix supported by single permeable layers (Fig. 5 a & c).
- Simulations show that decreasing permeabilities refer to the closure and constriction of effective conduits while matrix permeability mainly maintains constant indicated by similar fluid pressure fields in the matrix (Fig. 5 b & c).

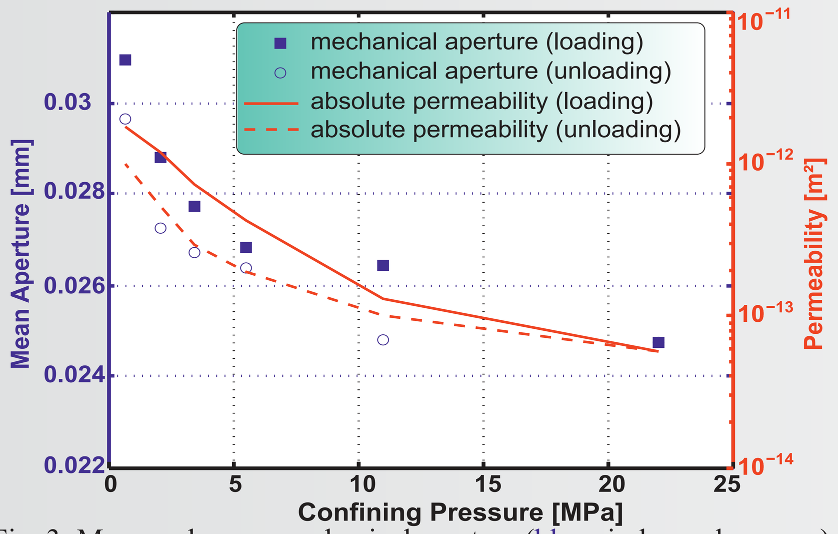

Fig. 3: Measured mean mechanical aperture (blue circles and squares) and absolute permeabilities (red lines) of the sample at loading and unloading conditions. Apertures are determined by applying the missing attenuation method on CT scans.

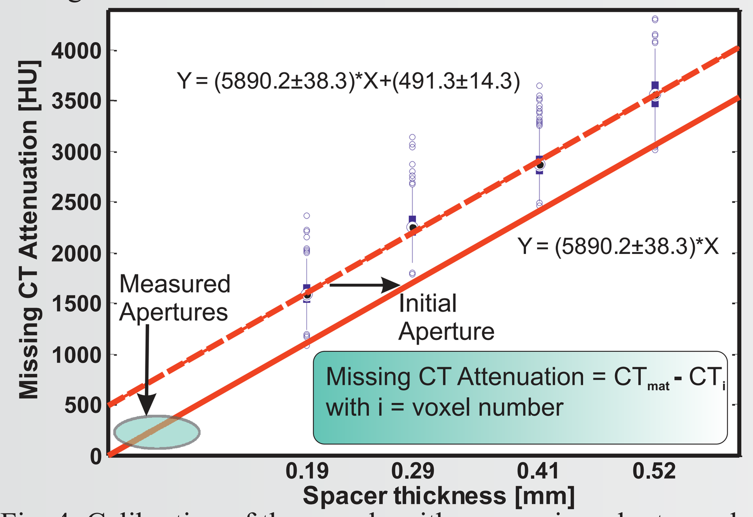

Fig. 4: Calibration of the sample with spacers in order to apply the missing attenuation method. The solid red line corresponds to fracture aperture while the dotted line corresponds to x-axes of spacer thickness. Thin/Thick blue lines show 25/75% confidence intervals. Empty circles represent outliers (after [3]).

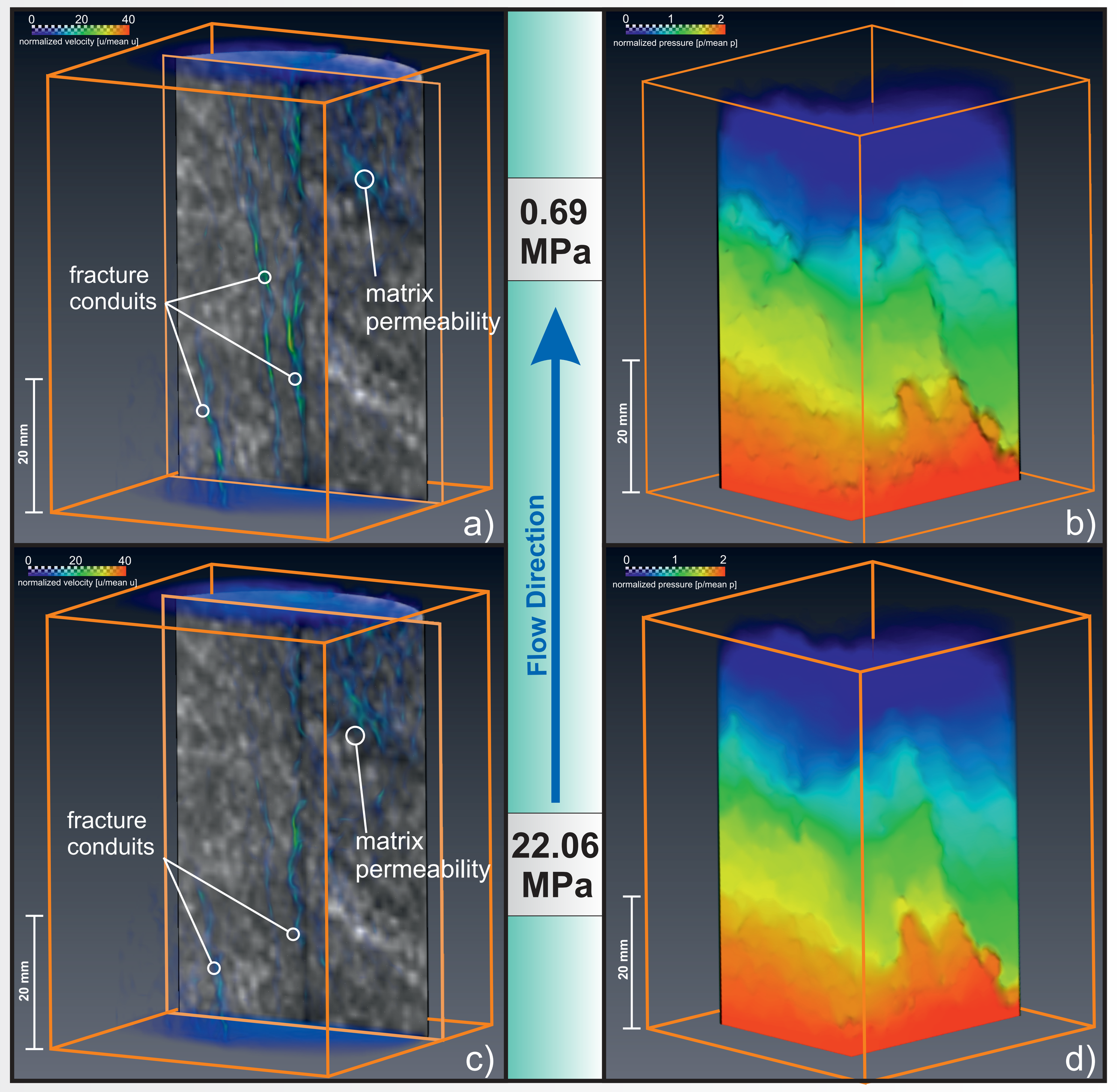

Fig. 5: Visualized 3D results of the LB forward simulation at confining pressures of 0.69 MPa (a,b) and 22.06 MPa (c,d). Fluid flow is visualized by fluid velocity per voxel normalized by the mean fluid velocity at the given pressure stage (a,c). On the right-hand side (b,d), fluid pressure inside the rock matrix which is also normalized is shown. Fluid flows from the bottom up.

4. Conclusions and future work

- Missing attenuation method, generally, is applicable to process CT data and to transfer them into a LB simulation.
- Experimental data can be approximately reproduced.
- Imprecisions probably rely on the relatively low resolution of the CT scanner (voxel dimension 0.5 x 0.5 x 1 mm³).
- Fluid flow in the sample is mainly based on fracture permeability and occurs along single and small conduits.
- Aperture distribution and connectivity of the conduits depends on the effective stress field.

Future Work

- Further simulations for remaining loading and unloading cycles are planned.
- Finding solutions to reduce imprecisions (adjusting calibration line).
- More precise consideration of fracture apertures due to increasing and decreasing stresses.

5. References

[1] GeoDict software programm package: Developed by Frauenhofer ITWM and distributed by Math2Market GmbH, Kaiserslautern, Germany, http://www.geodict.com.
[2] Huo, D. & Benson, S.M. (2014): An experimental investigation of stress-dependent permeability hysteresis behavior in rock fractures. AGU monograph: Dynamics of flow and transport in fractured porous media - Recent advances and future directions (under review).
[3] Huo, D., Pini, R. & Benson S.M (2014): Measurement of fracture aperture using CT scanning technique. Journal of Geophysical Research (under review).
[4] Ketcham, R.A., Slottke D.T. & Sharp Jr., J.M. (2010): Three-dimensional measuremnt of fractures in heterogeneous materials using high-resolution computed tomography. Geosphere, 6, pp.499-514.
[5] Landry, J.L. & Karpyn, Z.T. (2012): Single-phase lattice Boltzmann simulations of pore-scale flow in fractured permeable media. International Journal of Oil, Gas and Coal Technology, 5 (2/3), pp.182-206.
[6] Zimmerman, R.W. & Bodvarsson, G.S. (1996): Hydraulic conductivity of rock fractures. Transport in Porous Media, 23, pp. 1-30.